Oxygen Diffusion in Glassy Polymer Films: Effects of Other Gases and Changes in Pressure

Lars Poulsen and Peter R. Ogilby*

Department of Chemistry, Aarhus University, DK-8000 Århus, Denmark

Received: September 27, 1999; In Final Form: January 3, 2000

Sensitized singlet oxygen phosphorescence has been used to quantify oxygen diffusion in polystyrene and poly(methyl methacrylate) films. Prompted by unexplained results from previous studies (*Macromolecules* **1994**, *27*, 7041−7048; *Can. J. Chem.* **1995**, *73*, 1831−1840), the present experiments have been performed to better characterize the behavior of this photophysical probe of oxygen diffusion under a variety of conditions. Specifically, at total pressures less than 500 Torr, the effects of pressure changes and added nitrogen gas on the measured oxygen diffusion coefficient, singlet oxygen phosphorescence intensity, and rate constant for sensitizer quenching by oxygen have been examined. The results indicate that there is a "low" pressure domain in which the oxygen diffusion coefficient depends both on the oxygen pressure and on the pressure of an added copenetrant. Data obtained are discussed within the context of the dual-mode sorption theory.

Introduction

The study of gas diffusion in glassy polymers continues to be a topic of interest for both the scientific and technological communities.[1−4] The diffusion and sorption of oxygen, in particular, is important to those interested in polymer oxidative degradation, protective coatings, and packaging materials, among other practical applications. From a more fundamental perspective, many aspects of the mechanism(s) by which a polymer either inhibits or facilitates gas transport have yet to be fully understood. In all cases, an essential requirement is access to accurate diffusion coefficients that can be recorded under a variety of experimental conditions using easily characterized samples prepared in a reproducible manner.

Several years ago, we developed a spectroscopic technique to quantify oxygen diffusion coefficients in polymer films.[5−7] In this approach, oxygen sorption into the polymer is monitored using the near-infrared phosphorescence of singlet delta oxygen as a probe [$O_2(a^1\Delta_g) \rightarrow O_2(X^3\Sigma_g^-) + h\nu$]. Our method has several desirable features: (1) Comparatively small samples can be used. At present, the area probed is on the order of 2−4 mm^2 for samples that are ∼10−30 μm thick. (2) Because gas sorption is monitored, we are not adversely susceptible to pinholes in the sample. (3) We directly obtain the diffusion coefficient, D, and do not need to consider the gas solubility, S. (4) Polymer films can either be free standing or cast on a substrate. (5) Diffusion coefficients can be obtained over a wide temperature range.

In our studies thus far, singlet oxygen has been produced by energy transfer to ground state oxygen, $O_2(X^3\Sigma_g^-)$, from a triplet state sensitizer dissolved in the polymer. In this system, the intensity of $O_2(a^1\Delta_g)$ phosphorescence, I_Δ, is proportional to the quantum yield of phosphorescence, ϕ_p, which in turn is proportional to the quantum yield of singlet oxygen production, ϕ_Δ.

$$I_\Delta = \gamma \phi_\Delta k_r \tau_\Delta \tag{1}$$

The product $k_r\tau_\Delta$ is the fraction of $O_2(a^1\Delta_g)$ that decays via the radiative channel, where k_r is the a → X radiative rate constant and τ_Δ is the overall $O_2(a^1\Delta_g)$ lifetime in the polymer film. Although the product $k_r\tau_\Delta$ is, in general, very small (∼10^{-4}−10^{-5}),[8,9] the signal-to-noise levels experimentally obtained for I_Δ nevertheless make the technique viable. The proportionality constant γ includes instrumental parameters that account for signal collection efficiency and amplification, for example.

In a triplet-photosensitized system, the singlet oxygen quantum yield, ϕ_Δ, is proportional to the fraction of sensitizer triplet states quenched by oxygen

$$\phi_\Delta = \phi_T \frac{k_q[O_2]}{k_q[O_2] + \tau_T^{-1}} F_\Delta \tag{2}$$

where k_q is the rate constant for oxygen quenching of the sensitizer triplet state, τ_T is the triplet state lifetime in the absence of oxygen, ϕ_T is the triplet state quantum yield, and F_Δ is the fraction of quenching events that yield $O_2(a^1\Delta_g)$. Thus, when $k_q[O_2] \lesssim \tau_T^{-1}$, the intensity of singlet oxygen phosphorescence, I_Δ, will depend on the ground state oxygen concentration in the sample, $[O_2]$.

For the triplet-sensitized production of $O_2(a^1\Delta_g)$, I_Δ does not vary with $[O_2]$ over a wide range of oxygen concentrations.[5,10] Nevertheless, in many glassy polymers where k_q can be small, certainly in comparison to that found in liquids, changes in I_Δ can be used to quantify changes in $[O_2]$. The latter is particularly true when low concentrations of oxygen are incorporated into a previously degassed sample. This is illustrated by the data shown in Figure 1, where I_Δ is used to monitor oxygen sorption into a polystyrene film. It is important to recognize, in this regard, that our spectroscopic probe is responding to changes in the amount of sorbed oxygen that arise from very subtle changes of ∼0−100 Torr in the atmosphere surrounding the sample. This is in contrast to other measurements where the sample may experience pressure changes of over 10^4 Torr.[11]

Data such as those shown in Figure 1 can be analyzed to directly yield the oxygen diffusion coefficient, D, by using a

* To whom correspondence should be addressed.

10.1021/jp993449r CCC: $19.00
Published on Web 03/01/2000

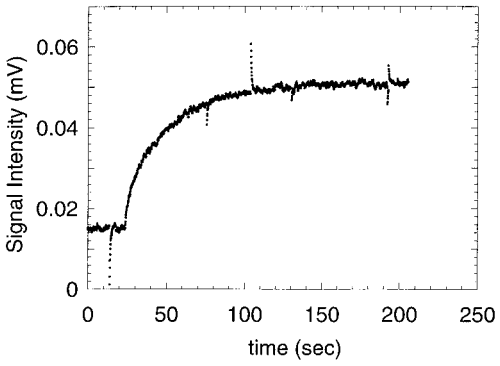

Figure 1. Singlet oxygen phosphorescence intensity, I_Δ, recorded as oxygen is sorbed into a 23 μm thick polystyrene film cast onto a glass substrate. *meso*-Tetraphenylporphine was used as the $O_2(a^1\Delta_g)$ sensitizer. These data were recorded upon exposure of a degassed film to 30 Torr of oxygen. The spikes on the trace are the response of the germanium detector to adventitious cosmic rays.

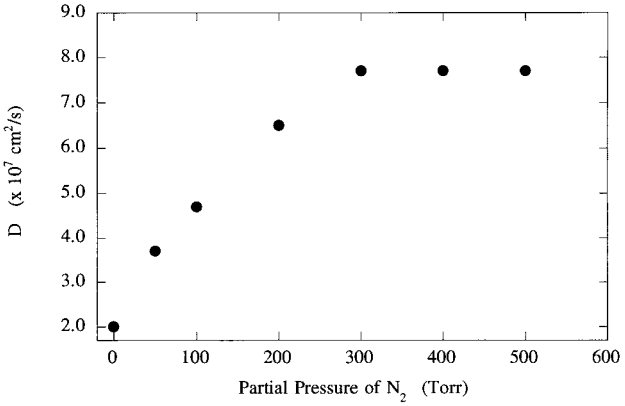

Figure 2. Plot of the oxygen diffusion coefficient, *D*, for a 25 °C polystyrene sample as a function of the partial pressure of nitrogen in the ambient atmosphere. The data were recorded at an oxygen pressure of 30 Torr. The data are from ref 7.

solution to Fick's second law for one-dimensional diffusion (eq 3).[5,6,12]

$$\frac{M_t}{M_\infty} = 1 - \sum_{n=0}^{\infty} \frac{8}{(2n+1)^2\pi^2} \exp\left(\frac{-D(2n+1)^2\pi^2 t}{4l^2}\right) \quad (3)$$

where M_t and M_∞ represent the amount of oxygen sorbed at times t and ∞, respectively. The sample thickness, l, can be quantified in independent experiments.

In some of our earlier studies, we examined the effect of added gases on the oxygen diffusion coefficient, *D*, in polystyrene and polycarbonate.[6,7] All experiments were performed at total pressures well below 760 Torr (1 atm). Values of *D* were recorded for polymer samples exposed to ambient oxygen atmospheres that contained varying pressures of nitrogen, helium, or argon. Furthermore, diffusion coefficients obtained as a function of temperature were used to obtain diffusion activation energies from Arrhenius plots of ln *D* against 1/*T*. Several interesting observations were made in these studies: (1) At a given temperature, the measured oxygen diffusion coefficient increased with an increase in the pressure of the added gas, asymptotically approaching a value of *D* approximately 4−5 times greater than that obtained in the absence of the added gas (Figure 2). These increases in the oxygen diffusion coefficient were independent of whether the diffusion coefficient of the added gas was greater than that of oxygen (e.g., He) or less than that of oxygen (e.g., N_2). (2) With one exception (vide infra), Arrhenius plots of the diffusion coefficient obtained with different pressures of added gas were parallel, suggesting negligible plasticization of the polymer by the added gas (Figure 3). However, the intercepts of the Arrhenius plots increased in a manner consistent with the overall increase in *D* as shown in Figure 2. Only the data recorded from polycarbonate samples with nitrogen as the added gas showed a slight change in the Arrhenius activation energy suggesting that, in this case, plasticization of the polymer by the added gas could be occurring. Although a number of possible interpretations were presented for these observations,[7] the discussion still had a rather large component of speculation.

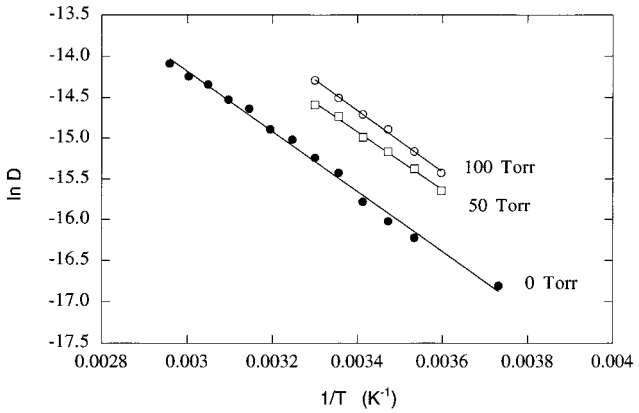

Figure 3. Plots of ln *D* vs 1/*T* for oxygen diffusion coefficients in polystyrene. Data were recorded under conditions in which the ambient atmosphere contained 30 Torr of O_2 and 0 Torr of added N_2 (●), 30 Torr of O_2 + 50 Torr of N_2 (□), and 30 Torr of O_2 + 100 Torr of N_2 (○). The solid lines are linear least-squares fits to the data. The data are from ref 7.

In an attempt to further elucidate these observations, we set out to perform a series of independent experiments. In particular, we felt that it was necessary to better understand the effect of pressure changes on the oxygen−organic molecule photosystem in a glassy polymer exposed to low ambient pressures (<760 Torr). In glassy polymers, there is significant evidence to suggest that gas sorption can be described in terms of two separate populations of sorbed molecules, the so-called Langmuir and Henry components, each of which has a different pressure dependence.[11,13−15] Although for many gas−polymer systems evidence of such dual-mode behavior may not become apparent until comparatively high ambient pressures are used (e.g., $\sim 10^3-10^4$ Torr),[11] it is not unreasonable to expect that dual-mode behavior can also be observed at pressures less than 760 Torr. In this article, we present experiments designed to ascertain how both our photophysical probe and *D* respond to changes in pressure and the presence of an added gas in the pressure domain <760 Torr.

Experimental Section

The time evolution of oxygen sorption was monitored using a singlet oxygen spectrometer that has previously been described.[5] Briefly, the singlet oxygen sensitizer was irradiated using a steady state 150 W xenon lamp whose output was passed through the following optical elements in succession: (1) a water filter, (2) Schott KG IR-removing filters, and (3) an Oriel model 77250 monochromator. Singlet oxygen phosphorescence was detected through a 1270 nm interference filter using a 77 K intrinsic germanium detector (North Coast model EO817L). Because of constraints set forth by the geometry of the sample chamber, the detector was aligned along the axis of excitation. This configuration requires that great care be exercised in

removing not just infrared components but unabsorbed UV/vis components from the excitation source so as not to saturate the detector with unwanted signal (UV/vis light not absorbed by the sensitizer can result in significant near-IR emission from optical elements used to spectrally isolate singlet oxygen phosphorescence[16]). The apparatus used to monitor time-resolved triplet absorption signals has likewise been described.[17]

The sample under study was placed in an evacuable, variable-temperature chamber fitted with windows suitable for optical experiments (modified Specac model 21000 sample chamber). This chamber was connected to a vacuum line which, in turn, was connected to cylinders of oxygen and nitrogen, or any other desired gas. Gases were delivered into the vacuum manifold through needle valves. Pressures were monitored using an MKS Baratron capacitance manometer. Coldfingers and gas reservoirs judiciously placed on the vacuum manifold facilitated mixing of two different gases prior to expansion into the sample chamber. The volume of the sample chamber was sufficiently large that the ambient pressure did not change as gases were sorbed into the sample.

Polystyrene and poly(methyl methacrylate) (PMMA) films with thicknesses in the range 10−30 μm were prepared by spin-casting using a Headway model EC101DT-R790 photoresist spinner. Benzene was used as the solvent for polystyrene and 2-butanone as the solvent for PMMA. In a typical preparation, ∼5 g of the polymer was dissolved in ∼12 mL of the solvent. Dissolution was slow and it took several days before an homogeneous solution was obtained. A solution of the sensitizer in the same solvent was then added, and this mixture was then cast onto a glass plate rotating at 7000 rpm. Sensitizer concentrations were adjusted such as to yield an absorbance of ∼0.3−0.5 at the excitation wavelength in the final film. Films were dried under an atmosphere of nitrogen for 24 h and then under vacuum for 48 h to ensure complete solvent removal. Samples were also annealed (50 °C, 1 h) to minimize differences in free volume that might have occurred with different rates of solvent removal.

Thicker PMMA samples (0.4 ± 0.1 mm) were obtained by cutting and polishing rods that had been prepared by bulk free-radical polymerization.[18,19] Briefly, methyl methacrylate (Aldrich) was distilled to remove the inhibitor. A mixture of methyl methacrylate, the sensitizer (acridine), and the radical initiator (1,1′-azobis(cyclohexanecarbonitrile), Aldrich) was degassed using three freeze−pump−thaw cycles and then sealed into an ampule. The ampule was placed into a 40 °C oil bath. After 1 h, the temperature was raised to 50 °C where it was kept for 12 h. The viscous samples were then slowly shaken and then kept at 70 °C for 24 h before raising the temperature to 90 °C for a final 12 h period. The absorption spectrum of acridine in the PMMA sample was identical to that recorded in a liquid solvent indicating that the sensitizer was indeed not influenced by the free radical polymerization.

Results and Discussion

1. Oxygen Sorption Studies. *1a. Diffusion Coefficients and Diffusion Activation Barriers.* For polystyrene samples prepared in this study, we obtain an oxygen diffusion coefficient, *D*, at 25 °C of (4.0 ± 0.1) × 10^{-7} cm^2 s^{-1} upon exposure of a degassed film to 30 Torr of oxygen. This value is slightly larger than that previously obtained by us using the same technique, *D*(25 °C) = (2.3 ± 0.2) × 10^{-7} cm^2 s^{-1},[5−7] and likely reflects differences in the materials used in each study. We likewise observe only a slight difference between the Arrhenius activation barrier obtained in the present study, E_{act} = 32 ± 1 kJ/mol, and that previously obtained, 30 ± 1 kJ/mol.[6,7]

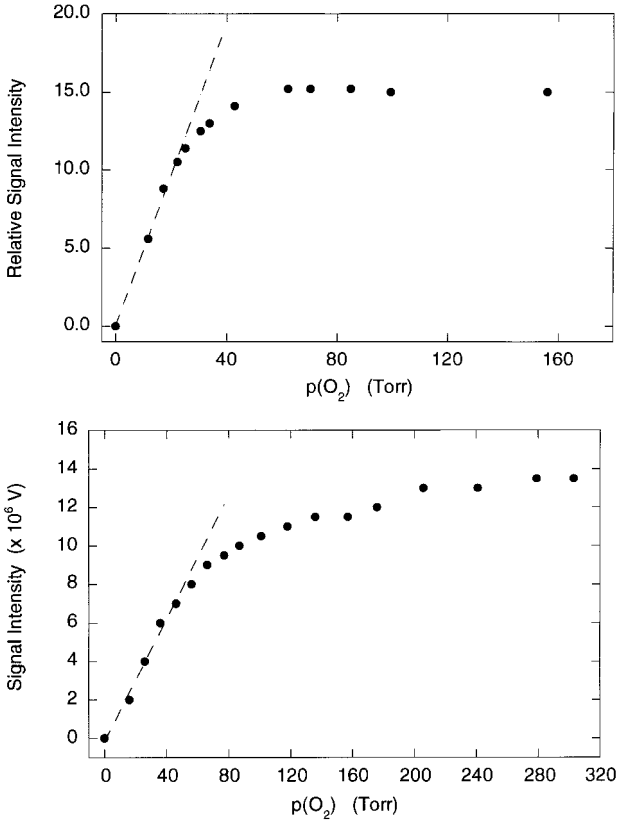

Figure 4. Plot of the sensitized $O_2(a^1\Delta_g)$ phosphorescence intensity, I_Δ^{eq}, vs the ambient oxygen pressure, $p(O_2)$, for samples that are in equilibrium with the ambient atmosphere. Values of I_Δ^{eq} were obtained from data such as those shown in Figure 1 using the signal intensity at the asymptote where I_Δ no longer changes with time. (a, top) TPP-sensitized $O_2(a^1\Delta_g)$ production in polystyrene. The dashed line is a linear fit to the first four data points. The data are from ref 5. (b, bottom) Rose-Bengal sensitized $O_2(a^1\Delta_g)$ production in PMMA. The dashed line is a linear fit to the first five data points.

For PMMA, we obtain *D*(25 °C) = (4.3 ± 0.9) × 10^{-8} cm^2 s^{-1} upon exposure of a degassed film to 50 Torr of oxygen. This number agrees well with those obtained from other studies, certainly given the expected differences in sample history and material; *D*(20 °C) = 3.8 × 10^{-8} cm^2 s^{-1},[20] *D* = 3.7 × 10^{-8} cm^2 s^{-1},[21] *D* = 3.3 × 10^{-8} cm^2 s^{-1},[22] and *D*(22 °C) = (1.4 ± 0.3) × 10^{-8} cm^2 s^{-1}.[23] As discussed below, however, it is likely that our *D* value of 4.3 × 10^{-8} cm^2 s^{-1} in PMMA is slightly larger than the true value.

1b. Pressure Dependence of the $O_2(a^1\Delta_g)$ Intensity for a Polymer Sample at Equilibrium with the Ambient Atmosphere. For polymer samples exposed to low ambient oxygen pressures, such that the concentration of sorbed oxygen is low, the intensity of the sensitized $O_2(a^1\Delta_g)$ phosphorescence signal, I_Δ, will be proportional to the concentration of sorbed oxygen (eqs 1 and 2). For a given sensitizer in a given polymer *at equilibrium* with the ambient atmosphere, plots of I_Δ^{eq} vs the ambient oxygen pressure indicate the pressure range over which our technique can be used to quantify oxygen diffusion (Figure 4).

At sufficiently low pressures, plots of I_Δ^{eq} vs the ambient oxygen pressure, $p(O_2)$, may be approximated by a linear function (Figure 4). Thus, for degassed samples exposed to an oxygen pressure in this domain, sorption data such as those shown in Figure 1 can be used directly with fitting routines based on eq 3 to obtain *D*. However, for degassed samples exposed to higher pressures, the time-dependent sorption data must be corrected for the nonlinearity of the I_Δ^{eq} vs $p(O_2)$ plot.

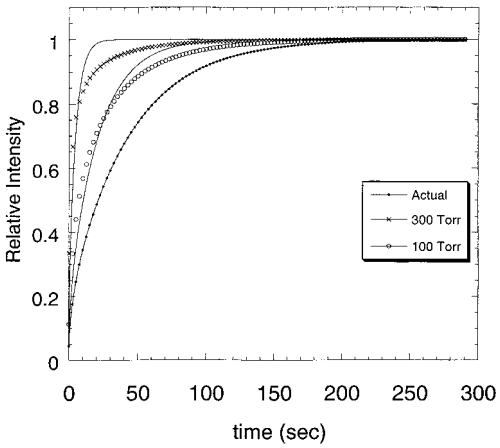

Figure 5. Simulated plots of oxygen sorption into a 15 μm thick PMMA sample. Using the data in Figure 4b, the simulation was performed for sorption into a degassed sample upon exposure to a specific ambient oxygen pressure. Under conditions where I_Δ^{eq} is linearly dependent on $p(O_2)$, the agreement between the simulated sorption (●) and the fit based on eq 3 (—) is excellent. At pressures where I_Δ^{eq} is no longer linearly dependent on $p(O_2)$, the simulated sorption curves (○ and ×) can no longer be represented by eq 3 (—).

Failure to make this correction can yield diffusion coefficients that are abnormally large. This source of error can be simulated and illustrated using published models.[12,24] In Figure 5, we show simulated oxygen sorption profiles for data that would be recorded upon exposure of a 15 μm thick PMMA sample to different ambient oxygen pressures (see Figure 4b for the I_Δ^{eq} vs $p(O_2)$ plot). At low oxygen pressures, the simulated data are well represented by the solution to Fick's second law for one-dimensional diffusion (eq 3).[12] At higher ambient oxygen pressures, where plots of I_Δ^{eq} vs $p(O_2)$ exhibit curvature, eq 3 no longer accurately describes the simulated data, yielding diffusion coefficients that are much larger than the true value. The pressure dependence of this deviation from the true diffusion coefficient is shown in Figure 6a, where D values obtained from fits of eq 3 to the simulated sorption data are plotted against the ambient oxygen pressure.

Given these simulations, it is important to now examine the effect of a change in the ambient oxygen pressure on the value of D experimentally obtained under conditions where I_Δ^{eq} does not depend linearly on $p(O_2)$. Without correcting for the I_Δ^{eq} vs $p(O_2)$ curvature, we find that D values obtained from fits of eq 3 to the sorption data indeed increase with an increase in $p(O_2)$ as predicted (Figure 6b). If this observed increase in D with $p(O_2)$ is due solely to a fitting artifact and there is no true molecular component to this phenomenon, then the value $D(\text{PMMA}) = (4.3 \pm 0.9) \times 10^{-8}$ cm^2 s^{-1} obtained upon exposure to 50 Torr of oxygen (vide supra) should be slightly larger than the true D value. Unfortunately, it is not trivial to accurately correct for curvature in plots of I_Δ^{eq} vs $p(O_2)$ which, in turn, would make it possible to obtain D from sorption curves recorded at higher ambient oxygen pressures.

2. Time-Resolved Triplet Absorption Studies. If the quenching of the triplet state sensitizer by oxygen occurs at or near the diffusion-controlled limit in the polymer, then pressure-dependent changes in the oxygen diffusion coefficient, D, will be reflected with a corresponding change in k_q, the rate constant for sensitizer quenching by oxygen. Such pressure-dependent changes in k_q are pertinent on two counts. In the first, it is essential to ascertain whether the addition of a copenetrant or a change in the ambient pressure can alter the intensity of the $O_2(a^1\Delta_g)$ phosphorescence signal as a consequence of the change

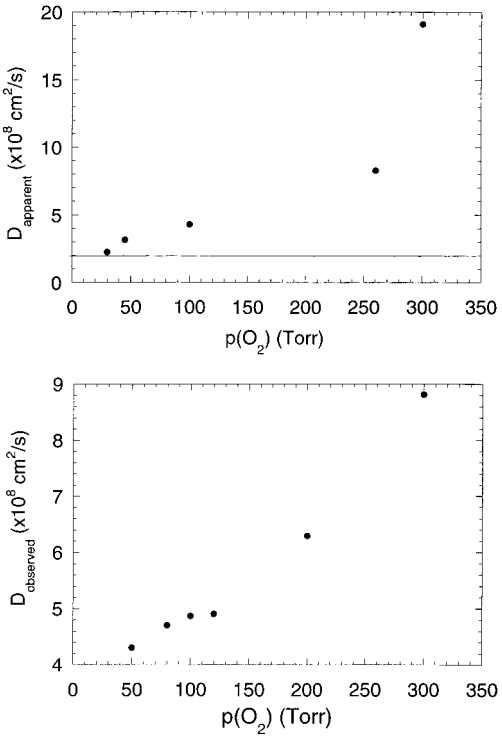

Figure 6. (a, top) Plot of the apparent oxygen diffusion coefficient, D, against the oxygen pressure surrounding a PMMA sample. Values of D were obtained by fitting eq 3 to simulated oxygen sorption data (see Figure 5). The solid line represents the diffusion coefficient that would be obtained if I_Δ^{eq} depended linearly on $p(O_2)$ over the entire pressure range. (b, bottom) Plot of D against the oxygen pressure surrounding a PMMA sample. In this case, values of D were obtained by fitting eq 3 to experimental oxygen sorption data recorded from a 20 μm thick PMMA sample doped with Rose-Bengal.

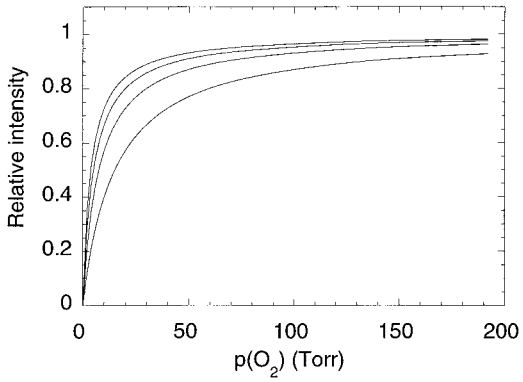

Figure 7. Simulation of the $O_2(a^1\Delta_g)$ phosphorescence intensity, I_Δ^{eq}, as a function of the oxygen partial pressure in equilibrium with the polymer sample. Intensity profiles were calculated using eq 2 with k_q values that varied by a factor of 4 (uppermost curve = largest k_q).

in k_q (eqs 1 and 2). For a sample in equilibrium with the ambient atmosphere, the effect of a pressure-dependent change in k_q on I_Δ^{eq} is modeled in Figure 7. The calculations show that even subtle changes in k_q can alter the pressure range over which our sorption probe can yield accurate diffusion coefficients. Second, if k_q is indeed directly proportional to D because sensitizer quenching occurs at the diffusion-controlled limit, then experiments to quantify k_q should provide a method to independently verify D data recorded from singlet oxygen phosphorescence experiments.

2a. Dependence of the Rate Constant for Sensitizer Triplet State Decay on the Ambient Oxygen Pressure. In time-resolved absorption experiments, the triplet state of *meso*-tetraphenyl-

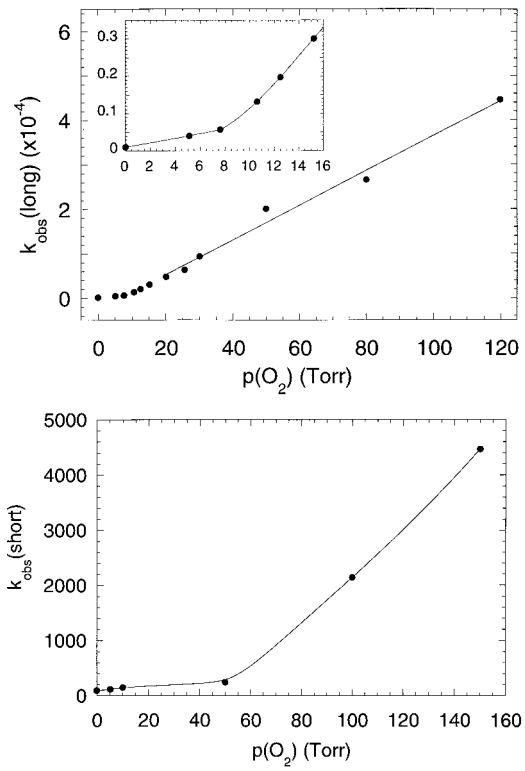

Figure 8. Plot of the observed first-order rate constant for triplet state quenching by oxygen as a function of the ambient oxygen partial pressure. Rate constants were obtained from a fit of eq 4 to the time-resolved triplet absorption signals. (a, top) Slow component (k_2) of the biexponential fit for signals recorded from the TPP triplet in polystyrene (15 μm thick sample). The solid line is a linear least-squares fit over the range 20−120 Torr. The insert shows data recorded at lower pressures. (b, bottom) Fast component (k_1) of the biexponential fit for signals recorded from the acridine triplet in PMMA at low $p(O_2)$. The solid line is an arbitrary function used simply to illustrate the curvature in this plot.

porphine (TPP) in polystyrene was monitored at 450 nm and the triplet state of acridine in PMMA was monitored at 440 nm. In both cases, the decay of the absorption signals did not follow first-order kinetics. This is a common observation in glassy polymers and is usually discussed in terms of triplet states that occupy a distribution of different sites in the polymer matrix.[18] One way to quantify such data is to fit the decay signals with a biexponential function

$$\Delta A = K[\exp(-k_1 t) + \exp(-k_2 t)] \qquad (4)$$

where ΔA is the change in sample absorbance due to the triplet state.

Upon equilibration of the polymer sample with an ambient atmosphere that contains oxygen, rate constants for both the fast (k_1) and slow (k_2) decay components increase (Figure 8). Moreover, plots of either k_1 or k_2 against $p(O_2)$ show the same trend. At low oxygen pressures (less than ∼12 Torr in polystyrene and ∼60 Torr in PMMA), the rate at which k_1 and k_2 increases with an increase in $p(O_2)$ is much less than the rate of increase at high oxygen pressures (i.e., plots of either k_1 or k_2 against $p(O_2)$ show pronounced curvature). At oxygen pressures greater than ∼12 Torr in polystyrene and ∼60 Torr in PMMA, the plots of k_1 and k_2 against $p(O_2)$ are linear (Figure 8).

Taking the solubility of oxygen in polystyrene to be $(7.8 \pm 1.6) \times 10^{-3}$ M/atm and in PMMA to be $(8.7 \pm 1.7) \times 10^{-3}$ M/atm,[23,25] one can generate corresponding plots of k_1 and k_2 against $[O_2]$. At any given $[O_2]$, the slope of such a plot represents the bimolecular rate constant for triplet state quenching by oxygen, k_q. The magnitude of k_q obtained from the fast decay component differs from that obtained from the slow decay component, which is consistent with the model of triplet states sorbed in a distribution of matrix sites each of which exhibits a different susceptibility to oxygen quenching. For data recorded at oxygen pressures greater than ∼12 Torr in polystyrene, the fast component yields a k_q value of $(8.1 \pm 1.6) \times 10^7$ s^{-1} M^{-1} whereas the slow component yields $k_q = (3.7 \pm 0.7) \times 10^7$ s^{-1} M^{-1}. For data recorded at oxygen pressures greater than ∼60 Torr in PMMA, values of k_q are a factor of ∼20 smaller [e.g., k_q(fast) $= (3.9 \pm 0.9) \times 10^6$ s^{-1} M^{-1}].

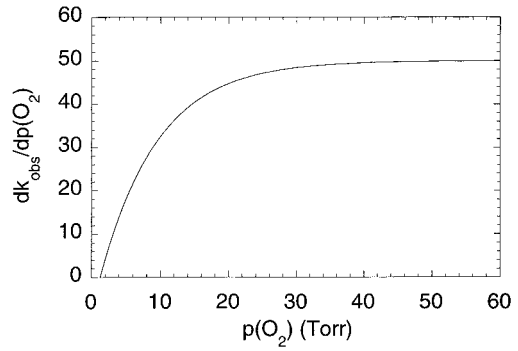

Figure 9. Plot of $dk_{obs}/dp(O_2)$ against $p(O_2)$, where k_{obs} is the first-order rate constant for oxygen quenching of the triplet sensitizer in polystyrene as shown in Figure 8. The derivative, $dk_{obs}/dp(O_2)$ is proportional to the bimolecular quenching rate constant k_q that, in turn, is proportional to the oxygen diffusion coefficient, D.

The magnitude of these bimolecular rate constants indicates that k_q should indeed be directly proportional to the oxygen diffusion coefficient in the polymer. For example, the average of the fast and slow rate constants for quenching in polystyrene (vide supra) is $\sim 6 \times 10^7$ s^{-1} M^{-1}. This number should represent a mean susceptibility for triplet state quenching by oxygen. Data from independent studies indicate that k_q is generally smaller than that for a diffusion-controlled reaction, k_{diff}, by a factor based on spin statistics.[26−28] Moreover, in a glassy polymer, where the influence of the oxygen-sensitizer charge-transfer state can be more pronounced,[29] k_q may be approximately $^4/_9$ that of k_{diff}.[23] Thus, when divided by the factor $^4/_9$, the average value $k_q \sim 6 \times 10^7$ s^{-1} M^{-1} corresponds to a diffusion-controlled rate constant, k_{diff}, for an oxygen-dependent process in polystyrene of $\sim 1.4 \times 10^8$ s^{-1} M^{-1}. Indeed, quenching rate constants obtained in a variety of independent studies[19,30,31] indicate that k_{diff} for a process involving oxygen in polystyrene is $\sim(1-2) \times 10^8$ s^{-1} M^{-1}. Thus, bimolecular rate constants for oxygen quenching of the sensitizer triplet state, k_q, are expected to be directly proportional to the oxygen diffusion coefficient, D.

The data in Figure 8 show that, at comparatively low oxygen ambient pressures, k_q is much *smaller* than that at high $p(O_2)$ values. Similar behavior has previously been observed for oxygen quenching of the bromopyrene triplet in an epoxy resin.[32] Thus, we infer that D at these lower oxygen pressures is smaller than that at higher pressures. This point can be illustrated in a different way for data such as those shown in Figure 8 by plotting the derivative of the ordinate with respect to the abscissa, $dk_{obs}/dp(O_2)$, against $p(O_2)$ (Figure 9).

In conclusion, the data indicate that, in the low-pressure limit, D increases with $p(O_2)$ under conditions where the total ambient pressure is also changing. As moderate pressures are approached (e.g., ∼15 Torr in polystyrene), D no longer changes with an increase in $p(O_2)$. The latter observation indicates that the

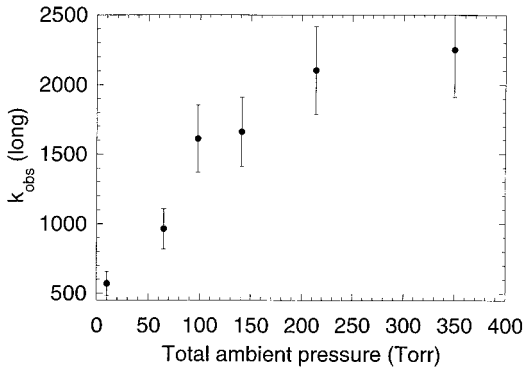

Figure 10. Plot of the pseudo first-order rate constant, k_{obs}, for the quenching of triplet TPP by oxygen (slow component, k_2) as a function of the total ambient pressure. The data were recorded from a polystyrene sample exposed to a constant oxygen partial pressure of 10 Torr but with varying pressures of added nitrogen gas.

oxygen sorption data shown in Figure 6b indeed reflect an artifact of the analysis.

2b. Time-Resolved Triplet Absorption Studies: Effect of Oxygen and an Added Copenetrant at a Constant Total Pressure. Time-resolved triplet state absorption experiments were performed on TPP in polystyrene at an ambient total pressure of 120 Torr. In these experiments, the oxygen partial pressure was varied over the range 0−40 Torr while maintaining a constant total pressure with nitrogen as the buffer gas.

In this case, we find that the rate constants for triplet state decay do not depend as strongly on $p(O_2)$ as they do in the absence of an added gas (Figure 8). The data nevertheless indicate that D increases with an increase in $p(O_2)$ reaching a threshold above which further changes in D do not occur. Above approximately 10 Torr $p(O_2)$, the bimolecular rate constants obtained from these quenching plots were the same as for the pure oxygen studies described above (section 2a).

2c. Time-Resolved Triplet Absorption Studies: Effect of Oxygen and an Added Copenetrant at a Variable Total Pressure. Time-resolved TPP triplet state absorption experiments were performed in polystyrene at a constant $p(O_2)$ of 10 Torr but at a total pressure that varied from 10 to 350 Torr. Again, nitrogen was used as the buffer gas. This experiment corresponds to the oxygen sorption experiment that yielded the data shown in Figure 2.

In this case, the rate constants obtained from the biexponential fit (eq 4) increase with $p(N_2)$ at low total pressures, and appear to level-off at higher pressures (Figure 10). Because $p(O_2)$ is held constant in all cases, data points correlate directly with the bimolecular rate constant for oxygen quenching of the triplet state and, in turn, D. Thus, the data in Figure 10 indicate that the oxygen diffusion coefficient indeed increases with an increase of the copenetrant pressure. This observation is completely consistent with that independently obtained from our oxygen sorption experiments (Figure 2). It is important to note that, in both our oxygen sorption and triplet absorption experiments, these pressure-dependent changes in D are observed over a wide pressure range of added gas (∼300 Torr).

3. **Summary of Experimental Data**. On the basis of the results presented in sections 1 and 2, we must distinguish between "high" and "low" oxygen pressure domains when discussing the pressure dependence of the oxygen diffusion coefficient D:

(1) At comparatively high oxygen pressures (greater than ∼12 Torr in polystyrene and ∼60 Torr in PMMA), D does not appear to change with a change in $p(O_2)$. Moreover, at these pressures, the data indicate that D is independent of $p(O_2)$ both when the total ambient pressure is changed and when the total pressure is kept constant using nitrogen as a buffer

(2) At comparatively low oxygen pressures (less than ∼12 Torr in polystyrene and ∼60 Torr in PMMA), D does change. In this pressure domain, D increases with an increase in $p(O_2)$ in the absence of an added gas. D also increases with an increase in the pressure of an added gas at a constant $p(O_2)$. In both cases, D does not increase indefinitely, but rather asymptotically converges on a value above which further pressure-dependent increases are not observed.

To our knowledge, there is only one other experimental study that addresses the issue of oxygen diffusion in this pressure domain and in these materials. In 1962, Barker reported that in PMMA, D increased with an increase in $p(O_2)$ over the range ∼150−760 Torr, and in polycarbonate, D increased with an increase in $p(O_2)$ over the range ∼40−1000 Torr.[33] Clearly, our observations are not consistent with those of Barker's. In an attempt to rationalize this discrepancy, it should be pointed out that Barker used a rather indirect technique to monitor oxygen sorption. In this case, the polymers were irradiated with high energy electrons (i.e., γ-rays) to create F-centers which would then change color as oxygen was sorbed into the material. The notion was that oxygen sorption could then be quantified by monitoring the time evolution of this moving colored boundary. In his paper, however, Barker clearly notes limitations in the accuracy of his technique, including the fact that γ-radiation results in the chemical degradation of the material under study. Thus, it is possible that Barker's pressure-dependent results reflect more than just the simple diffusion of oxygen.

In a more recent report, Compañ et al.[34] monitored the permeability of oxygen in films of semicrystalline linear low-density polyethylene. In this case, oxygen diffusion coefficients obtained from time-lag measurements were also found to increase with the oxygen pressure over the range 150−950 Torr. The semicrystalline material used in this study, however, is significantly different from that used in our study, and it is not unreasonable to expect pressure-dependent changes in D to occur in slightly different pressure domains.

Finally, we have already mentioned (vide supra, section 2a) that the pressure dependence we reported in Figure 8 is consistent with results from an analogous triplet absorption study in an epoxy resin.[32]

4. **Interpretation: Dual-Mode Sorption**. The observed distinction between high- and low-pressure domains is consistent with the dual-mode model of gas sorption.[11,13−15] In liquids and polymer rubbers, gas sorption behaves according to Henry's law in which the mole fraction of a dissolved gas depends linearly on the partial pressure of that gas in the atmosphere surrounding the sample. In amorphous glasses, however, gas sorption does not often behave according to Henry's law, and a second pressure-dependent term is commonly added to the Henry's law term to account for this deviation. Specifically, there is a large body of sorption data that supports the use of a Langmuir-type sorption isotherm to model low-pressure behavior. The total concentration, c, of sorbed gas is then expressed as the sum of Henry (H) and Langmuir (L) terms both of which depend on the partial pressure, p, of the gas surrounding the sample.

$$c = K_H p + K_L \frac{bp}{1 + bp} \tag{5}$$

The Langmuir term is believed to describe gas sorption in cavities or voids that are unique to a glassy material (i.e., a

static free volume),[7] and b in eq 5 is a void affinity constant. For penetrants that have a comparatively large void affinity constant, the pressure-dependent distinction between Langmuir and Henry domains will become apparent at much lower pressures. At higher pressures, "Henry behavior" is typically observed in that the amount of sorbed gas depends linearly on the ambient pressure, and this is likewise represented in eq 5. The overall gas diffusion coefficient will thus reflect the diffusion of both the Henry and Langmuir populations.

Many of our results are indeed consistent with this dual-mode sorption model. At low oxygen pressures, oxygen diffusion is retarded, which is consistent with immobilization in the Langmuir sites. As the oxygen pressure is increased and more of the Langmuir sites become occupied, the diffusion coefficient likewise increases. When the Langmuir sites become saturated, the diffusion coefficient remains constant and is dominated by the Henry population. Likewise, the increase in the oxygen diffusion coefficient upon addition of a copenetrant could reflect the simple displacement of oxygen by the copenetrant from Langmuir sites that hinder gas propagation.[7] In other words, oxygen and the copenetrant compete for the available Langmuir sites. In this regard, it is important to note two points: (1) the copenetrant-dependent increase in the oxygen diffusion coefficient, D, is independent of whether the diffusion coefficient of the added gas is larger or smaller than D, and (2) upon increasing the copenetrant pressure, D increases until all of the oxygen is displaced from the Langmuir sites. When this point is reached, and the Langmuir sites are saturated with the copenetrant, further increases in the copenetrant pressure have no effect on D (Figures 2 and 10).

With respect to the experiments involving a copenetrant, it has been suggested[13] that the displacement from the Langmuir cavities of one gas, such as oxygen, by another gas, such as nitrogen, would result in a decrease in the overall oxygen solubility. In principle, we could address this issue by using the intensity of our singlet oxygen phosphorescence signal to quantify the effect of an added gas on the relative solubility of oxygen. Specifically, values of I_Δ^{eq} obtained from data such as those shown in Figure 1 could be used in this regard. However, it is important to stress at this juncture that a number of variables influence I_Δ^{eq}, and thus one must proceed cautiously in making the direct connection between I_Δ^{eq} and the oxygen solubility. With this disclaimer in mind, we find that I_Δ^{eq} in fact *increases* slightly upon the addition of another gas, giving the appearance of an increase rather than a decrease in oxygen solubility.[7] This apparent increase in oxygen solubility could indicate a swelling or expansion of the polymer cavities that make up the static free volume and that, in turn, define the Langmuir term. Moreover, this swelling would not necessarily alter the dynamic motions that define the Arrhenius activation barrier for diffusion. Thus, Arrhenius plots recorded at various pressures of an added gas would be parallel, but displaced to yield a different intercept as shown in Figure 3. At present, it is clear that more experiments are needed to ascertain whether the observed increase in I_Δ^{eq} indeed accurately reflects a copenetrant-dependent increase in oxygen solubility.

Conclusions

This study was prompted by the results of previous experiments. Specifically, we had observed that, at pressures less than 500 Torr, the diffusion coefficient, D, of oxygen in a glassy polymer increased with an increase in the pressure of an added gas. Moreover, under these same conditions, the Arrhenius activation energy for diffusion remained constant indicating negligible plasticization of the polymer by the added gas. On the basis of these intriguing results, we set out to better characterize our photophysical probe for oxygen diffusion to ensure that we were not being deluded by an artifact.

We have ascertained that under some conditions, our probe for oxygen diffusion yields inaccurate data. Nevertheless, we also confirm that our previous observations are indeed accurate. Specifically, we have documented that at oxygen pressures less than ~50 Torr in polystyrene and PMMA, D increases with both an increase in the oxygen pressure and an increase in the pressure of an added gas. These data are consistent with the dual-mode model of gas sorption in glassy polymers. Our results should be pertinent not only in a number of practical applications (i.e., gas separation membranes, sensors) but should be useful to those interested in the kinetics of oxygen-dependent reactions in glassy polymers.

Acknowledgment. This work was supported by operating funds from Aarhus University.

References and Notes

(1) Vieth, W. R. *Diffusion In and Through Polymers*; Oxford University Press: New York, 1991.
(2) Kesting, R. E.; Fritzsche, A. K. *Polymeric Gas Separation Membranes*; John Wiley and Sons: New York, 1993.
(3) *Polymeric Gas Separation Membranes*; Paul, D. R., Yampol'skii, Y. P.; Eds.; CRC Press: Boca Raton, FL, 1994.
(4) *Diffusion in Polymers*; Neogi, P., Ed.; Marcel Dekker: New York, 1996.
(5) Gao, Y.; Ogilby, P. R. *Macromolecules* **1992**, *25*, 4962−4966.
(6) Gao, Y.; Baca, A. M.; Wang, B.; Ogilby, P. R. *Macromolecules* **1994**, *27*, 7041−7048.
(7) Wang, B.; Ogilby, P. R. *Can. J. Chem.* **1995**, *73*, 1831−1840.
(8) Ogilby, P. R. *Acc. Chem. Res.* **1999**, *32*, 512−519.
(9) Scurlock, R. D.; Mártire, D. O.; Ogilby, P. R.; Taylor, V. L.; Clough, R. L. *Macromolecules* **1994**, *27*, 4787−4794.
(10) Kristiansen, M.; Scurlock, R. D.; Iu, K.-K.; Ogilby, P. R. *J. Phys. Chem.* **1991**, *95*, 5190−5197.
(11) Koros, W. J.; Chern, R. T.; Stannett, V.; Hopfenberg, H. B. *J. Polym. Sci.: Polym. Phys. Ed.* **1981**, *19*, 1513−1530.
(12) Crank, J. *The Mathematics of Diffusion*, 2nd ed.; Oxford Press: Oxford, UK, 1975.
(13) Koros, W. J. *J. Polym. Sci.: Polym. Phys. Ed.* **1980**, *18*, 981−992.
(14) Paul, D. R. *Ber. Bunsen-Ges. Phys. Chem.* **1979**, *83*, 294−302.
(15) Zhou, S.; Stern, S. A. *J. Polym. Sci.: B: Polym. Phys.* **1989**, *27*, 205−222.
(16) Scurlock, R. D.; Iu, K.-K.; Ogilby, P. R. *J. Photochem.* **1987**, *37*, 247−255.
(17) Keszthelyi, T.; Weldon, D.; Andersen, T. N.; Poulsen, T. D.; Mikkelsen, K. V.; Ogilby, P. R. *Photochem. Photobiol.* **1999**, *70*, 531−539.
(18) Clough, R. L.; Dillon, M. P.; Iu, K.-K.; Ogilby, P. R. *Macromolecules* **1989**, *22*, 3620−3628.
(19) Ogilby, P. R.; Dillon, M. P.; Kristiansen, M.; Clough, R. L. *Macromolecules* **1992**, *25*, 3399−3405.
(20) MacCallum, J. R.; Rudkin, A. L. *Eur. Polym. J.* **1978**, *14*, 655−656.
(21) Kaptan, Y.; Pekcan, Ö.; Arca, E.; Güven, O. *J. Appl. Polym. Sci.* **1989**, *37*, 2577−2585.
(22) Higashide, F.; Omata, K.; Nozawa, Y.; Yoshioka, H. *J. Polym. Sci.: Polym. Chem. Ed.* **1977**, *15*, 2019−2028.
(23) Charlesworth, J. M.; Gan, T. H. *J. Phys. Chem.* **1996**, *100*, 14922−14927.
(24) Yekta, A.; Masoumi, Z.; Winnik, M. A. *Can. J. Chem.* **1995**, *73*, 2021−2029.
(25) Peterson, C. M. *J. Appl. Polym. Sci.* **1968**, *12*, 2649−2667.
(26) Gijzeman, O. L. J.; Kaufman, F.; Porter, G. *J. Chem. Soc., Faraday Trans. 2* **1973**, *69*, 708−720.
(27) Garner, A.; Wilkinson, F. *Chem. Phys. Lett.* **1977**, *45*, 432−435.
(28) Redmond, R. W.; Braslavsky, S. E. *Chem. Phys. Lett.* **1988**, *148*, 523−529.

(29) Ogilby, P. R.; Sanetra, J. *J. Phys. Chem.* **1993**, *97*, 4689−4694.
(30) Scurlock, R. D.; Kristiansen, M.; Ogilby, P. R.; Taylor, V. L.; Clough, R. L. *Polym. Degrad. Stab.* **1998**, *60*, 145−159.
(31) Ogilby, P. R.; Kristiansen, M.; Mártire, D. O.; Scurlock, R. D.; Taylor, V. L.; Clough, R. L. *Adv. Chem. Ser.* **1996**, *249*, 113−126.
(32) Chu, D. Y.; Thomas, J. K.; Kuczynski, J. *Macromolecules* **1988**, *21*, 2094−2100.
(33) Barker, R. E. *J. Polym. Sci.* **1962**, *58*, 553−570.
(34) Compañ, V.; López-Lidón, M.; Andrio, A.; Riande, E. *Macromolecules* **1998**, *31*, 6984−6990.